International Journal of Applied Engineering Research ISSN 0973-4562 Volume 14, Number 24 (2019) pp. 4562-4572

Optimization of the Underwater Friction Stir Welding of Pipes Using Hybrid RSM-Fuzzy Approach

A. M. El-Kassas[1], Ibrahim Sabry[2]

[1]Department of Production Engineering and Mechanical Design, Faculty of Engineering, Tanta University, P.O. Box, Tanta 31512, Egypt. Email: ahmed.elkassas@f-eng.tanta.edu.eg

[2]Manufacturing Engineering Department, Modern Academy for Engineering and Technology, P.O. Box Cairo 11571, Egypt. Email: ibrahem.sabry@eng.modern-academy.edu.eg

Abstract

This is the first research to investigate the Underwater Friction Stir Welding of Pipes (UFSWoP). UFSWoP of Al 1050 pipes was carried out successfully by designing a new device that allows the underwater rotational motion of the pipe to be friction stir welded. An important consideration in the UFSWoP is the cooling effect on the surrounding water during the process. The water-cooling affects directly the mechanical properties of the produced joint. A study is carried out to conclude and predict the effects of the UFSWoP process parameters on the mechanical properties of the welded joint. A Box Behnken experimental design was employed with different levels of tool rotational speed, traverse speed and tool diameter. The corresponding response considered was the tensile strength of the produced joints. Finally, a hybrid Response Surface Methodology-Fuzzy based model was proposed and evaluated for predicting the considered response of the UFSWoP process. This model showed more accurate predicted results than the Artificial Neural Network based model.

Keywords: Underwater Friction Stir Welding of Pipes, Fuzzy, Response Surface Methodology.

I. INTRODUCTION

In 1991, Friction Stir Welding (FSW) was developed by the Welding Institute (TWI) [1]. FSW is a new solid-state welding method that uses a non-consumable tool without reaching the melting temperature of the welded materials. It is applicable to a wide range of materials from metals, even to polymers [2]. As it is not a fusion process, the nonexistence of defects like cracking, porosity, splatter, shrinkage … etc. is eligible. This generally improves the quality of the welded joints in terms of the mechanical properties. The heat generated by the tool causes the two facing base materials to be softened and plastic deformed as shown in Fig. 1.

Recently Underwater Friction Stir Welding (UFSW) has gained a special interest. UFSW has promising applications where applying the traditional fusion welding process is uphill. Also, the water cooling during the process is efficient in controlling the heat input to the joint. UFSW has merits over the FSW process (cf. [3]) and it has been reported that UFSW produce joints with better mechanical properties than other fusion welding processes and FSW itself [4, 5]. UFSW also yields a superior quality grain size welded joints in relatively short cycle time [6, 7].

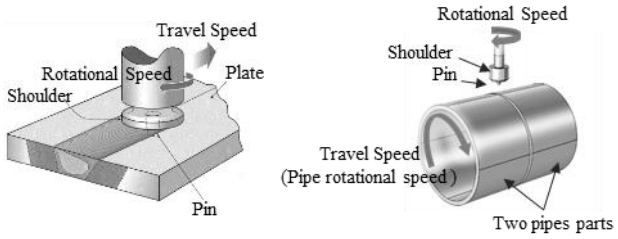

(a) FSW of plates process (b) FSW of pipes process

Figure 1 A schematic drawing of the friction stir welding process for (a) plates and (b) pipes.

Figure 1 The friction stir welding process.

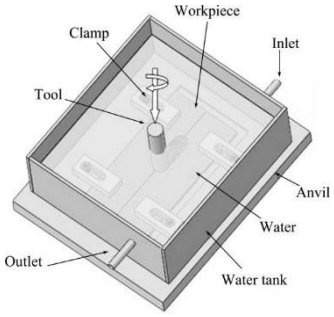

Figure 2 The UFSW of plates process.

Welding of pipes is a very special case from the welding perspective view. This is done conventionally using the fusion welding processes [8]. As stated earlier, the demerits of the fusion welding lead to lowering the mechanical properties of the welded pipes [9]. So, investigating the FSW of pipes was inevitable. Unluckily, due to the different

obstructions in the FSW of pipes, limited studies have been performed to weld pipes using the FSW process [10, 11].

Small diameter AA6061 pipes were friction stir welded by a threaded pin cylindrical tool with by Lammlein et al. [12]. They also achieved a maximum weld efficiency of 70% at a rotational speed of 1600 rpm and 355 mm/min as traverse speed. Another study [13] considered the FSW of AA6061 pipes using a tapered pin. The welded joint's tensile strength was about 62% of the base metal at conditions of 630 rpm and 1 mm/s as rotational speed and travel speed respectively. The FSW of Stainless-steel pipes was considered in [14] while Hattingh et al. [15] investigated the semiautomatic FSW of Aluminum 6082 tubes. AA6063 pipes butt joints were considered for studying the effect of rotational and traverse speed by Ismail et al. [16]. While in [17], a lap joint was performed by the FSW of two pipes using triangular frustum shaped pin. The optimum conditions of the process were 40 mm/min for travel speed and a rotational speed of 600 rpm and 800 rpm. On the other side, two pipes with dissimilar metals (aluminum and copper) with thicknesses 1.5 and 1 mm were friction stir welded [18]. A tool with a tilt angle was used to enhance the joint quality measured in the tensile strength and hardness.

This paper investigates the UFSW of pipes (UFSWoP) process. To the best of our knowledge, the UFSWoP has never been carried out before in the literature. So, the literature review in this paper is divided into two sections. The preceding one was to review the FSW of pipes in the air as no previous studies of the FSW of pipes underwater. And the following part is on reviewing the UFSW studies which all of them performed for welding the plates only.

A detailed research work on UFSW technique was performed in [19] to increase the mechanical properties of the AA6061 welded joints. The UFSW of AA2014-T4 was also experimented and the tensile strength of the produced joint was successfully improved to a 75% of the base material [20]. In [21], an improvement in the UFSW produced joint was achieved and also in the hardness except of the nugget zone. The effects of the UFSW process parameters were also investigated. The lower tool rotational speed leaded to a higher tensile strength of the UFSW joint of the AA2519-T87 alloy [22]. However, the lowest hardness value is increased by the increase of the traverse speed for the same alloy [23].

The UFSW of two dissimilar joints of AA6061 and AA7075 was carried out in [24]. The effects of two process parameters: the rotational speed and traverse speed were investigated considering the produced joint's grain size and hardness. Higher traverse speed and lower rotational speeds resulted in finer grain size and larger hardness. An empirical model is constructed based on regression method. This model predicted the experimental values obtained considerably [24]. Only a limited number of empirical models have been proposed to relate the welding joint quality with the UFSW process parameters [25]. Regression Analysis (RA) as an example was used to generate such models for the UFSW process [26]. Also, Response Surface Methodology (RSM) has been used extensively in optimizing he FSW process [27, 28, cf. 29]. In [30], RSM and Artificial Neural Networks (ANN) were used to predict the average grain size of the AA6061-T6 produced joint by UFSW process. The ANN model usually yields more accurate results compared to the RA and RSM model [30, 31].

This paper investigates the UFSWoP process for the first time and proposes a hybrid Response Surface Methodology-Fuzzy (RSM-Fuzzy) based model for the UFSWoP process. This model outperforms the generated ANN based model.

II. MATERIALS AND METHODS

2.1. EXPERIMENTAL SETUP OF THE UFSWOP

Generally, the FSW process of pipes begins with positioning the tool pin into the gap between the two facing pipes until the shoulder reaches the two pipes' surfaces (Fig. 1(b)). The UFSWoP has the same procedure of the FSW of pipes in addition to that it is performed underwater.

The UFSWoP process was conducted to join two pieces of Al 1050 pipes. Each pipe was 30 mm in outer diameter and 3 mm in thickness. Table 1 shows the chemical composition of the Al 1050 material of the pipes.

Table 1 Chemical composition (Wt. %) of Al 1050

Wt. %	Al	Si	Fe	Cu	Mn	Mg	Cr	Zn
	Bal	0.3	0.1	0.4	0.9	0.04	0.01	0.12

A hard tool steel non consumable tool was used with the following specification: a shoulder with diameter (D) and height 5 mm. The pin profile is tapered with initial diameter 5 mm and final diameter 1 mm with pin length is 3 mm. The used tool in shown in Fig. 3.

Initially, a vertical milling machine (VMM) was chosen to carry out the FSW of the pipes. The rotating motion of the pipes – which represent the traverse speed (s) – was allowed by using a chuck attached to the dividing head of the VMM and a tailing head. The dividing head is operated by a motor with inverter rather than manually.

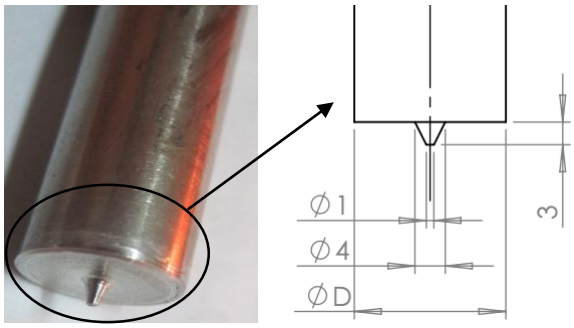

Figure 3 The used tool.

A robust fixture is needed for holding the two pipes and can be rotated with them. Our previous ideas and designs can be found in [34]. Our final design, which was used in this paper, was a fixture with a longitudinal full support to the pipes. The issue of disassembly of the two pipes after the welding was solved by splitting the fixture into two parts. Every part is securely attached to the other by locking rotating motion. The fixture design is indicated in Fig. 4(a). The whole fixture is enclosed in a rigid box while its ends protruded through holes with mechanical seals. This box has an inlet and outlet holes for the entry and the exit of water. The whole setup is shown in Fig. 4(b).

(a)

(b)

Figure 4 (a) the used fixture (b) the experimental setup.

2.2. DETERMINATION OF THE JOINT QUALITY

One of the produced welded pipes is photographed in Fig. 5. For measuring the considered responses, a tensile test for each specimen was conducted. Specimens for the tensile test were prepared as in Fig. 6 according to standard ASTM E8M-04 [32].

III. EXPERIMENTS AND MODELING

3.1. EXPERIMENTAL DESIGN

To study experimentally the process parameters' effects on the quality of the produced joints in the UFSWoP, the tool rotational speed (n), traverse speed (s) and the tool shoulder diameter (D) are considered. A lot of previous studies of the FSW generally [33] and our previous one of the FSW of pipes [34] reported that the tool rotational speed (n) and traverse speed (s) are significant parameters in the FSW of pipes. The effect of the tool shoulder diameter consideration has been studied in a limited number of previous FSW studies of plates [35]. So, its effect on the UFSWoP – which hasn't been studied before – is experimented here as an additional contribution of our work.

Figure 5 A welded pipe by the UFSWoP process.

Figure 6 A tensile test sample.

A different number of trial experiments were performed at different values of the considered UFSWoP's parameters. The chosen levels of the parameters were selected based on the quality of the produced joints expressed in the tensile strength of the joint. The experimented levels of the corresponding parameters are revealed in Table 2.

Table 2 UFSWoP parameters and their levels.

Parameter	Unit	Level		
		-1	0	1
Rotational speed (n)	rpm	710	980	1250
Traverse speed (s)	mm/min	100	200	300
Shoulder diameter (D)	mm	10	20	30

A Box Behnken experimental design was carried out to investigate the relation between the considered parameters and the response. Its corresponding design matrix is listed in Table 3. The use of such design induces carrying out a relatively lower number of experiments rather than normal factorial designs [36]. This creates higher order response surfaces and provides modelling of the response surface using a lower number of experiments [37].

Table 3 The matrix design of experiments.

Sample	n (rpm)	s (mm/min)	D (mm)
1	980	300	10
2	980	300	30
3	980	100	10
4	710	200	10
5	980	100	30
6	710	300	20
7	710	200	30
8	1250	200	10
9	980	200	20
10	980	200	20
11	710	100	20
12	1250	300	20
13	1250	200	30
14	1250	100	20
15	980	200	20

3.2. RESPONSE SURFACE METHODOLOGY

Response Surface Methodology (RSM) is an optimization technique that is composed of statistical and mathematical methods. It is efficient when the output response is influenced by a number of parameters [38]. In RSM, the response can be represented as a function of the considered parameters as in Eq. (1). This function is defined using regression analysis.

$$Y = \Phi(x_1, x_2, x_k) \pm \varepsilon \quad (1)$$

The function Φ is called the response surface. It is a polynomial equation form which can be linear or non-linear based on the model's nature. Y is the output response and x_i is the ith considered parameter when the number of the considered parameters is k. The experimental errors are represented in Eq. (1) by the residual error (ε). It is calculated by the sum of square deviations between the experimental response and the estimated one. That leads to choosing the best equation for the considered model.

In our model, the considered response is the tensile strength of the joint. While, the three considered parameters are: $x_1 = n, x_2 = s$ and $x_3 = D$. A quadratic polynomial was chosen to predict the output response. The response defined by the second order polynomial model in terms of the considered parameters is expressed in Eq. (2).

As the model need to be significantly tested, ANOVA test is employed for the model. ANOVA is used to check if the model fits our experimental data or not.

$$T = \beta_0 + \sum_{i=1}^{3} \beta_i x_i + \sum_{i=1}^{3} \beta_{ii} x_i^2 + \sum_{i=1}^{3} \sum_{j=2,\ i<j}^{3} \beta_{ij} x_i x_j \quad (2)$$

T is the considered response which is the joint's tensile strength. β_0 is the intercept, β_i, β_{ii} and β_{ij} are the linear, quadratic and interaction coefficients, respectively.

3.3. FUZZY LOGIC

Fuzzy logic is a pure mathematical tool which its use is favorable if all input values are uncertain [39]. The input data can be ordinary scalar, vectors, matrices and strings as well as fuzzy number. Also, they could be an output of another model. However, to implement the fuzzy logic, the input parameters must be in the form of a fuzzy set. The fuzzy set is primarily a crisp set for which an element is either a member of it or not. A set of linguistic rules is the backbone of the fuzzy system. The general working module of a fuzzy system is shown in Fig. 7. A fuzzy system generally begins with the fuzzification phase where the input values are fuzzified using the membership functions. Then, a knowledge base (IF-THEN) generates a fuzzy output set based on the fuzzy input [40]. Finally, the fuzzy output is finally defuzzified to get the final output. The final phase of the defuzzification can be carried out by different methods [cf. 41].

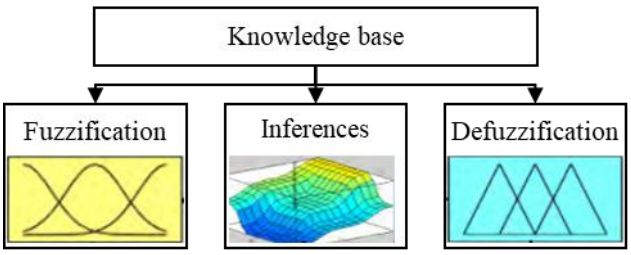

Figure 7 Fuzzy system architecture.

In this study, the fuzzy model represents the relationship between the considered parameters and the response. The input parameters (the rotational speed, the traverse speed and the shoulder diameter) and the output variable (the joint's tensile strength) were used for the development of the fuzzy model. In the knowledge base development, the rules were constructed according to the experimental data. The fuzzy rule takes the form of a conditional statement:

IF x is F THEN y is R

x and y are linguistic variables representing the input and output variables respectively. While, F and R are linguistic values representing the input and output variables respectively.

3.4. HYBRID FUZZY-RSM METHOD

Increasing the number of fuzzy rules will level up the efficiency and precision of the fuzzy model. However, that means an extra cost of larger number experimental samples. So, in this paper, the developed RSM model (relating the considered parameters with the joint's tensile strength) is used for generating more points to hopefully increase the efficiency of the fuzzy model. The layout of the hybrid Fuzzy-RSM model is shown in Fig. 8.

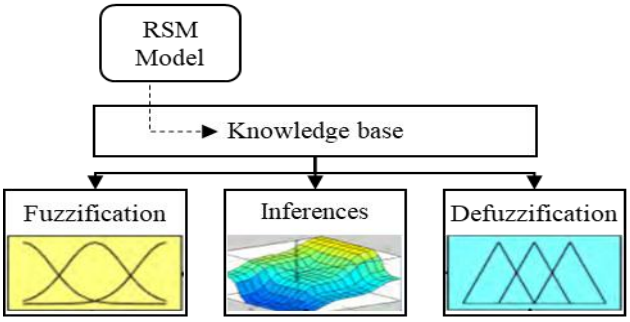

Figure 8 Hybrid Fuzzy-RSM system architecture.

IV. RESULTS AND DISCUSSION

4.1. THE RSM MODEL

4.1.1. MODELLING

The values of the RSM model coefficients for the considered response (the joint's tensile strength) were calculated using equations in [42] and presented in Table 4. The *P* values for each model coefficient, that determines if the coefficient contributes significantly to the model or not, are reported also.

Table 4 Calculated coefficients and their *P* values.

Term	*Coefficient*	*Value*	*P Value*
Linear	β_0	-159.3	0.004
n	β_1	0.3635	0.041
s	β_2	0.5883	0.001
D	β_3	2.948	0.998
Square			
n^2	β_{11}	- 0.000178	0.001
s^2	β_{22}	- 0.000844	0.005
D^2	β_{33}	- 0.0492	0.036
Interaction			
ns	β_{12}	- 0.000110	0.134
nD	β_{13}	- 0.000373	0.572
sD	β_{23}	- 0.00309	0.123

Based on the results in Table 4, all the linear terms are significant except the shoulder diameter. Whilst, all the square ones are significant at 95% confidence level. In addition, all the interaction terms don't affect significantly the response. So, the final uncoded model can be represented at Eq. (3).

$$T = -118.0 + 0.3339\,n + 0.4183\,s + 1.964\,D - 0.000178\,n^2 - 0.000844\,s^2 - 0.0492\,D^2 \quad (3)$$

ANOVA output of the regression model in Eq. (3) is tabulated in Table 5. It indicated the adequacy of the model (P value < 0.05) and the effectiveness of the model (Adjusted R^2 = 0.86). The ANOVA results indicated the model's goodness of fit (R^2 = 0.92) and the lack of fit is insignificant (P value = 0.066).

Table 5 ANOVA test results of the model in Eq. (3).

	df	*SS*	*MS*	*F* value	*P* value
Total	14	1669.8	–	–	–
Model	6	1536.4	256.1	15.36	< 0.001
Error	8	133.3	16.67	–	–
Lack of fit	6	130.4	21.7	14.6	0.066
Pure error	2	2.98	1.49	–	–
R^2	0.92	–	–	–	–
Adjusted R^2	0.86				

df: degree of freedom, *SS*: sum of squares, *MS*: mean square,

A residual analysis was also used for checking the adequacy of the RSM model. The residual results are plotted in Fig. 9. Fig. 9(a) shows the spreading of the residuals on almost a straight line which means a good correlation between the predicted and experimental values. Also, a minimum variance between the predicted and experimental ones are observed for the residuals versus the predicted values in Fig. 9(b). Positive and negative residuals, appear in Fig. 9(c), assure the existence of the correlation and finally Fig. 9(d) reveals clearly the adequacy of the RSM developed.

4.1.2. INFLUENCE OF PROCESS PARAMETERS

Before proceeding to the optimization of the UFSWoP, the influence of the UFSWoP parameters on the considered response (joint's tensile strength) should be analyzed. 3D response surface graphs were generated for the three considered parameters and shown in Fig. 10(a-c). Also, 2D contour plots based on the model in Eq. (3) are shown in Fig. 10(d-f). Three plots are constructed by considering two parameters as variables and the third one as fixed in the middle level.

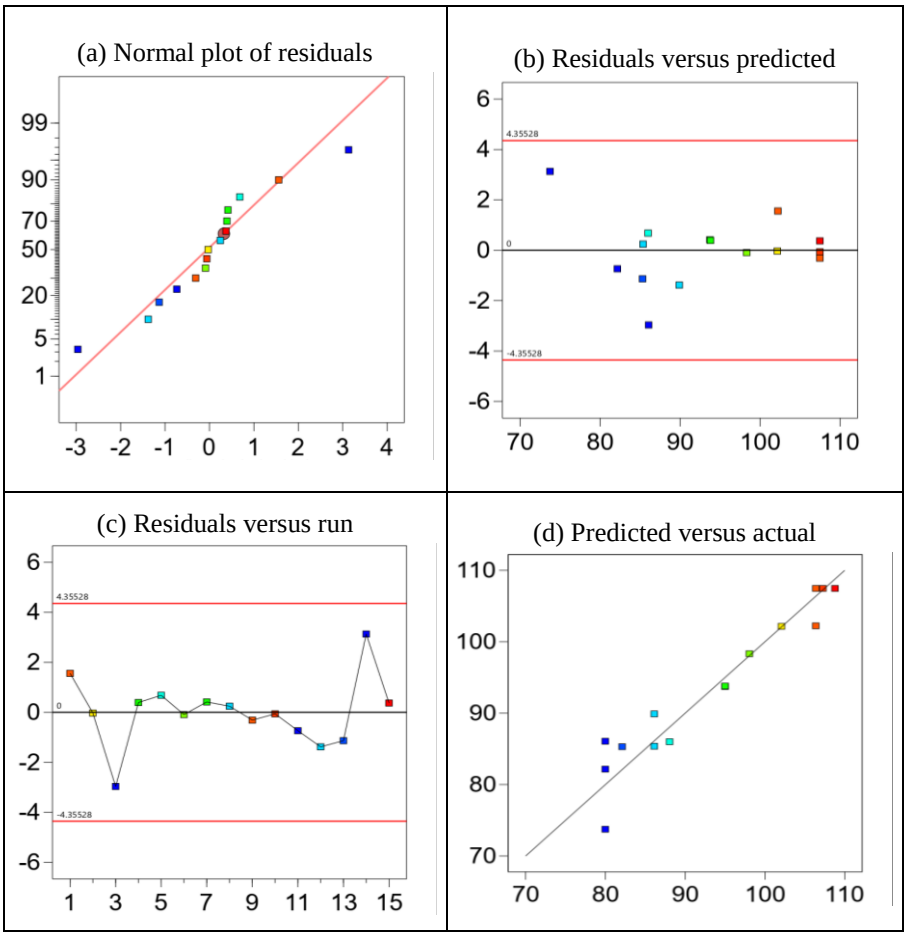

Figure 9 Plot of residuals (a) normal plot of the residuals, (b) residuals versus the predicted values, (c) residuals versus
experimental run, and (d) predicted versus actual values.

The influence of the rotational speed (n) on the tensile strength of the produced joint can be concluded from Fig. 10. The joint's tensile strength increases with the decrease in the tool rotational speed (n) until reaching a specific value and then the behavior is reversed. The value of 980 rpm acts as a transition point of the tensile strength with the tool rotational speed (n). At this rotational speed, the same trend with regard to the welding speed (s) can be visualized from Fig. 10. An optimum joint tensile strength can be obtained at 200 mm/min welding speed for the middle level of the tool rotational speed (n) and the shoulder diameter (D). Also, the increase in the welding speed (s) value increases the tensile strength of the joint only out of the 980 rpm range. However, the resultant tensile strength is relatively low due to the dominant effect of the tool rotational speed (n).

The shoulder diameter (D) hasn't a significant effect on the joint's tensile strength. However, a value of 20 mm will yield a relatively high tensile strength of the produced joint in the corresponding ranges.

4.1.3. OPTIMIZATION

The RSM model was successfully optimized to maximize the joint's tensile strength. For the RSM model, the best solution for maximization corresponds to rotational speed of 940 rpm, traverse speed of 240 mm/min and shoulder diameter of 17.6 mm. These parameters based on the RSM model yield a joint's tensile strength of 109.4 MPa.

4.2. THE FUZZY MODEL

4.2.1. MOEDLLING

Each fuzzy role creates a relationship in a fuzzy region. The fuzzy regions are defined by the membership functions. In this paper, the fuzzy modeling is employed by Gaussian functions for the process parameters. Gaussian function has high efficiency in assigning the membership value to the element [43]. While, the joint's tensile strength is defined by the triangular function which increases and decreases progressively with single value only [44].

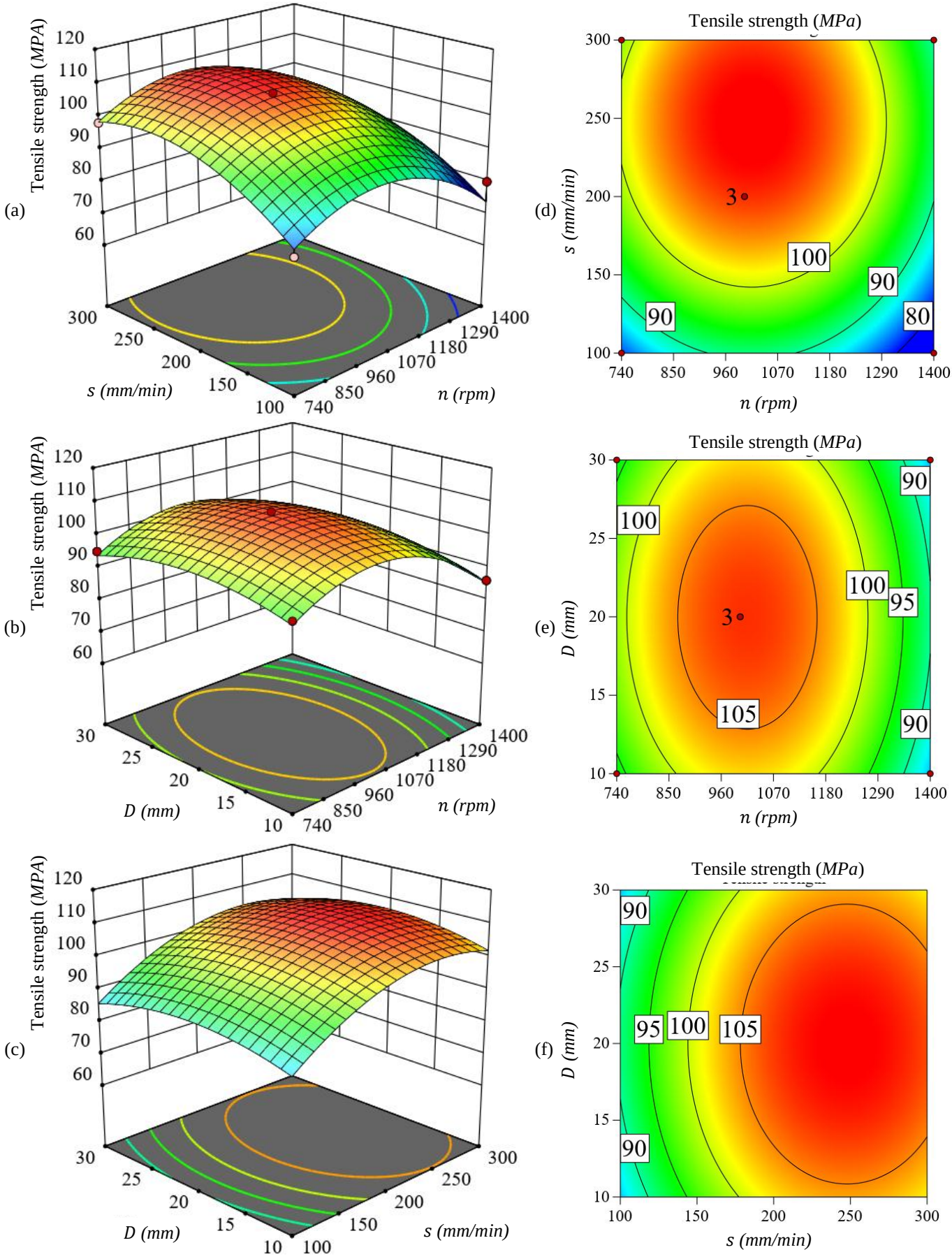

Figure 10 (a, b, c) surface graphs and (d, e, f) 2D contour plots corresponding to a, b and c, respectively.

In the experimental work, each parameter had only three levels so, it couldn't be presented in more than three membership functions. So, for every considered parameter, three membership functions were applied: low (L), medium (M) and high (H). The output response (the joint tensile strength) was employed with five membership functions: bad (B), acceptable (A), good (G), very good (V) and excellent (E). Membership functions for input and output are shown in Fig. 11. As 15 experimental points were carried out and the 3 repeated points from the experiments were averaged to represent a single fuzzy point. Thus, a set of 12 rules were as follows:

R1: IF n is M AND s is H AND D is L THEN T is E
R2: IF n is M AND s is H AND D is H THEN T is VG
R3: IF n is M AND s is L AND D is L THEN T is B
R4: IF n is L AND s is M AND D is L THEN T is G
R5: IF n is M AND s is L AND D is H THEN T is A
R6: IF n is L AND s is H AND D is M THEN T is VG
R7: IF n is L AND s is M AND D is H THEN T is G
R8: IF n is H AND s is M AND D is L THEN T is A
R9: IF n is M AND s is M AND D is M THEN T is E
R10: IF n is L AND s is L AND D is M THEN T is B
R11: IF n is H AND s is H AND D is M THEN T is A
R12: IF n is H AND s is M AND D is H THEN T is B
R13: IF n is H AND s is L AND D is M THEN T is B

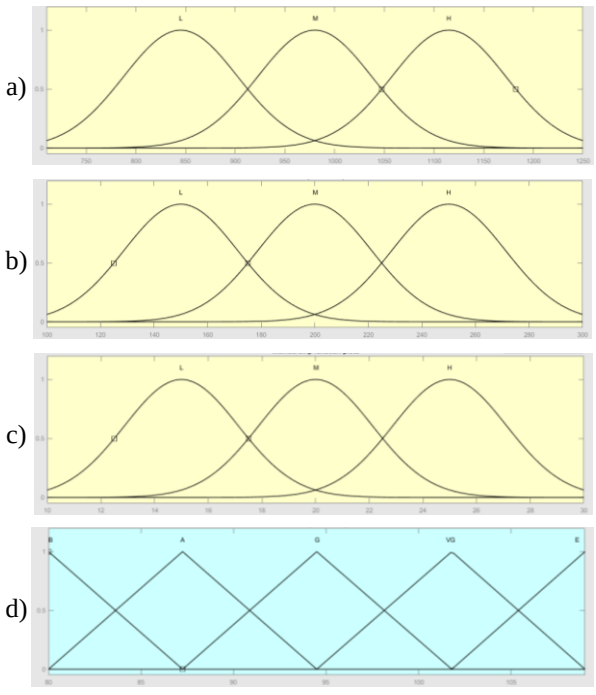

Figure 11 The membership function for a) rotational speed, b) traverse speed, c) shoulder diameter and d) joint's tensile strength.

In our model the method of centroid of area was implemented as a defuzzification method as it gives accurate results rather than other defuzzification methods [45].

4.2.2. OPTIMIZATION

Figure 12 shows the input parameters' values resulting in the maximum joint's tensile strength. Based on the fuzzy model, the maximum joint's tensile strength resulted by a value of 980 rpm, 200 mm/min and 20 mm for the rotational speed, traverse speed and shoulder diameter respectively. These values are almost the experiment no. 15 of the experiments performed which means that the fuzzy model is more accurate than the RSM in prediction. Unfortunately, the limited availability of the data usually results in high error and affect the prediction efficiency badly.

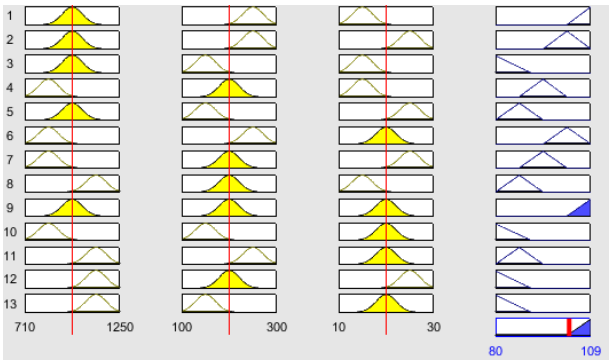

Figure 12 Fuzzy reasoning for maximization of the joint's tensile strength.

4.3. THE HYBRID FUZZY-RSM MODEL

4.3.1. MOEDLLING

For three levels of parameters, a number of 27 combinations can be prepared as experiments. There were 13 points for the fuzzy logic model, so an additional 14 points were generated by the RSM model and were fed into the fuzzy system as rules as follows:

R14: IF n is L AND s is L AND D is L THEN T is A
R15: IF n is L AND s is L AND D is H THEN T is A
R16: IF n is L AND s is M AND D is L THEN T is VG
R17: IF n is L AND s is H AND D is L THEN T is VG
R18: IF n is L AND s is H AND D is H THEN T is VG
R19: IF n is M AND s is L AND D is M THEN T is G
R20: IF n is M AND s is M AND D is L THEN T is E
R21: IF n is M AND s is M AND D is H THEN T is E
R22: IF n is M AND s is H AND D is M THEN T is E
R23: IF n is H AND s is L AND D is L THEN T is B
R24: IF n is H AND s is L AND D is H THEN T is B
R25: IF n is H AND s is M AND D is M THEN T is G
R26: IF n is H AND s is H AND D is L THEN T is G
R27: IF n is H AND s is H AND D is H THEN T is G

4.3.2. OPTIMIZATION

Based on the RSM-Fuzzy model, the maximum joint's tensile strength is exactly the same as developed by the fuzzy logic model.

4.4. EVALUATING THE EMRICAL MODELS

Many tools are usually used to check the adequacy of the generated models with respect to the actual (experimental) data. The selected tools used for evaluating were the root mean square error (RMSE), Nash–Sutcliffe model efficiency coefficient (NSE), chi-square (χ^2) and the coefficient of the determination (R^2). Different indicators were calculated for the RSM and fuzzy models and tabulated in Table 6. An additional model for our problem was created based on an artificial neural network (ANN), which is described intensively in [46, 47], and was compared in Table 6 also.

It is clear from Table 6 that the fuzzy model has a near performance, but more adequate than the RSM model while the ANN model has a superior performance than both of them. However, the RSM-Fuzzy model exceeds the performance of all other RSM, Fuzzy and ANN models.

Table 6 The evaluation of empirical models developed.

	RMSE	NSE	χ^2	R^2
RSM	2.9995	0.9192	1.6014	0.92
Fuzzy	2.273	0.9595	1.6824	0.9343
ANN	1.8444	0.9694	0.5552	0.9719
RSM-Fuzzy	1.6094	0.9767	0.4243	0.9841

V. CONCLUSION

In this paper, a hybrid RSM-Fuzzy model was created for prediction and maximization the joint's tensile strength which produced by the Underwater Friction Stir Welding of Pipes (UFSWoP) process. A three factor with three levels Box Behnken experimental design was employed to construct empirical models based on the experimental data. The Response Surface Methodology (RSM) model revealed that the rotational speed and the traverse speed were the main significant factors affecting the joint's tensile strength while there is no significant effect of the shoulder diameter. The prediction accuracy of the constructed RSM and fuzzy models were investigated by statistical tests: the root mean square error, Nash–Sutcliffe model efficiency coefficient, chi-square and the coefficient of the determination. The fuzzy model showed slightly more efficiency than the RSM model, although a developed Artificial Neural Network (ANN) model for the problem exceeded the both of them. Thus, the developed RSM-Fuzzy could predict the joint's tensile strength precisely more than all of the other models: the RSM, fuzzy, ANN with higher coefficient of correlation ($R^2 = 0.98$). Finally, the optimal values of the considered parameters to maximize the joint's tensile strength obtained as: 980 rpm, 200 mm/min, 20 mm for the rotational speed, traverse speed and the shoulder diameter respectively.

REFERENCES

[1] TWI Ltd., "TWI Group websites," The Welding Institute, 29 March 2017. [Online]. Available: http://www.twi-global.com/capabilities/joining-technologies/friction-processes/frictionstir-welding

[2] Paramaguru, D., Pedapati, S. R., and Awang, M. (2019). A Review on Underwater Friction Stir Welding (UFSW). In *The Advances in Joining Technology* (pp. 71-83). Springer, Singapore.

[3] Wahid, M. A., and SIDDIQUEE, A. N. (2018). Review on underwater friction stir welding: a variant of friction stir welding with great potential of improving joint properties. *Transactions of Nonferrous Metals Society of China*, *28*(2), 193-219.

[4] Fratini, L., Buffa, G., and Shivpuri, R. (2010). Mechanical and metallurgical effects of in process cooling during friction stir welding of AA7075-T6 butt joints. *Acta Materialia*, *58*(6), 2056-2067.

[5] Zhang, H. J., Liu, H. J., and Yu, L. (2011). Microstructure and mechanical properties as a function of rotation speed in underwater friction stir welded aluminum alloy joints. *Materials & Design*, *32*(8-9), 4402-4407.

[6] Liu, H. J., Zhang, H. J., Huang, Y. X., and Lei, Y. U. (2010). Mechanical properties of underwater friction stir welded 2219 aluminum alloy. *Transactions of Nonferrous Metals Society of China*, *20*(8), 1387-1391.

[7] Wahid, M. A., Khan, Z. A., Siddiquee, A. N., Shandley, R., and Sharma, N. (2019). Analysis of process parameters effects on underwater friction stir welding of aluminum alloy 6082-T6. *Proceedings of the Institution of Mechanical Engineers, Part B: Journal of Engineering Manufacture*, *233*(6), 1700-1710.

[8] Na, S. J., and Lee, H. J. (1996). A study on parameter optimization in the circumferential GTA welding of aluminium pipes using a semi-analytical finite-element method. *Journal of materials processing technology*, *57*(1-2), 95-102.

[9] Jain, R., Kumari, K., Kesharwani, R. K., Kumar, S., Pal, S. K., Singh, S. B., ... and Samantaray, A. K. (2015). Friction stir welding: scope and recent development. In *Modern Manufacturing Engineering* (pp. 179-229). Springer, Cham.

[10] Iqbal, M. P., Jain, R., and Pal, S. K. (2019). Numerical and experimental study on friction stir welding of aluminum alloy pipe. *Journal of Materials Processing Technology*, 116258.

[11] El-Kassas, A. M., and Sabry, I. (2019). Using Multi Criteria Decision Making in Optimizing the Friction Stir Welding Process of Pipes: A Tool Pin Diameter Perspective. *International Journal of Applied Engineering Research*, *14*(18), 3668-3677.

[12] Lammlein, D. H., Gibson, B. T., DeLapp, D. R., Cox, C., Strauss, A. M., and Cook, G. E. (2012). The friction stir welding of small-diameter pipe: an experimental and numerical proof of concept for automation and manufacturing. *Proceedings of the Institution of Mechanical Engineers, Part B: Journal of Engineering Manufacture*, *226*(3), 383-398.

[13] Khanna, N., Bharati, M., Sharma, P., and Badheka, V. J. (2019). Design-of-experiments application in the friction stir welding of aluminium alloy AA 8011-h14 for structural application. *Multidiscipline Modeling in Materials and Structures*.

[14] Mahoney, M., Sanderson, S., Feng, Z., Steel, R., Packer, S., and Fleck, D. (2013). Friction stir welding of pipeline steels. In *Friction Stir Welding and Processing VII* (pp. 59-69). Springer, Cham.

[15] Hattingh, D. G., Von Welligh, L. G., Bernard, D., Susmel, L., Tovo, R., and James, M. N. (2016). Semiautomatic friction stir welding of 38 mm OD 6082-T6 aluminium tubes. *Journal of Materials Processing Technology*, *238*, 255-266.

[16] Ismail, A., Awang, M., and Samsudin, S. H. (2015). The influence of process parameters on the temperature profile of friction stir welded aluminium alloy 6063-T6 pipe butt joint. In *Mechanical and Materials Engineering of Modern Structure and Component Design* (pp. 243-249). Springer, Cham.

[17] Jamshidi Aval, H., and Falahati Naghibi, M. (2017). Orbital friction stir lap welding in tubular parts of aluminium alloy AA5083. *Science and Technology of Welding and Joining*, *22*(7), 562-572.

[18] Chen, B., Chen, K., Hao, W., Liang, Z., Yao, J., Zhang, L., and Shan, A. (2015). Friction stir welding of small-dimension Al3003 and pure Cu pipes. *Journal of Materials Processing Technology*, *223*, 48-57.

[19] Bloodworth, T. S. (2009). *On the immersed friction stir welding of AA6061-T6: a metallurgic and mechanical comparison to friction stir welding* (Doctoral dissertation, Vanderbilt University).

[20] Ghetiya, N. D., and Patel, K. M. (2018). Numerical simulation on an effect of backing plates on joint temperature and weld quality in air and immersed FSW of AA2014-T6. *The International Journal of Advanced Manufacturing Technology*, *99*(5-8), 1937-1951.

[21] Liu, H. J., Zhang, H. J., Huang, Y. X., and Lei, Y. U. (2010). Mechanical properties of underwater friction stir welded 2219 aluminum alloy. *Transactions of Nonferrous Metals Society of China*, *20*(8), 1387-1391.

[22] Sabari, S. S., Malarvizhi, S., and Balasubramanian, V. (2016). Characteristics of FSW and UWFSW joints of AA2519-T87 aluminium alloy: Effect of tool rotation speed. *Journal of Manufacturing Processes*, *22*, 278-289.

[23] Liu, H. J., Zhang, H. J., and Yu, L. (2011). Effect of welding speed on microstructures and mechanical properties of underwater friction stir welded 2219 aluminum alloy. *Materials & Design*, *32*(3), 1548-1553.

[24] Bijanrostami, K., and Vatankhah Barenji, R. (2019). Underwater dissimilar friction stir welding of aluminum alloys: Elucidating the grain size and hardness of the joints. *Proceedings of the Institution of Mechanical Engineers, Part L: Journal of Materials: Design and Applications*, *233*(4), 763-775.

[25] Wahid, M. A., Masood, S., Khan, Z. A., Siddiquee, A. N., Badruddin, I. A., and Algahtani, A. (2019). A simulation-based study on the effect of underwater friction stir welding process parameters using different evolutionary optimization algorithms. *Proceedings of the Institution of Mechanical Engineers, Part C: Journal of Mechanical Engineering Science*.

[26] Paramaguru, D., Pedapati, S. R., Awang, M., and Mohebbi, H. (2018, November). Mathematical Model to Predict Tensile Strength of Underwater Friction Stir Welded (UFSW) on 5052 Aluminium Alloys. In *ASME 2018 International Mechanical Engineering Congress and Exposition*. American Society of Mechanical Engineers Digital Collection.

[27] Periyasamy, Y. K., Perumal, A. V., and Periyasamy, B. K. (2019). Optimization of process parameters on friction stir welding of AA7075-T651 and AA6061 joint using response surface methodology. *Materials Research Express, 6*(9), 096558.

[28] Singh, H. N., Kaushik, A., and Juneja, D. (2019). Optimization of process parameters of friction stir welded joint of AA6061 and AA6082 by response surface methodology (RSM). *International Journal of Research in Engineering and Innovation, 3*(6), 417-427.

[29] Chanakyan, C., Sivasankar, S., Meignanamoorthy, M., Ravichandran, M., Alagarsamy, S. V., Kumar, S. D., and Sakthivelu, S. (2019). Friction stir processing (FSP) of numerical study based on design of experiment-review. *Materials Today: Proceedings*.

[30] Rathinasuriyan, C., Sankar, R., Shanbhag, A. G., and SenthilKumar, V. S. (2019). Prediction of the Average Grain Size in Submerged Friction Stir Welds of AA 6061-T6. *Materials Today: Proceedings*, *16*, 907-917.

[31] Sabry, I., Khourshid, A. M., Hindawy, H. M., and Elkassas, A. (2017). Comparison of RSM and RA with ANN in predicting mechanical properties of friction stir welded aluminum pipes. *Engineering and Technology in India*, *2*(1).

[32] Int, A.S.T.M. (2004). ASTM E8M-04, Standard Test Methods for Tension Testing of Metallic Materials.

[33] Singh, M. K., Porwal, R. K., and Mishra, S. (2020). Optimization-Related Studies on the Operational Parameters of Friction Stir Welding: An Overview. In *Trends in Manufacturing Processes* (pp. 1-9). Springer, Singapore.

[34] El-Kassas, A. M., and Sabry, I. (2019). Using Multi Criteria Decision Making in Optimizing the Friction Stir Welding Process of Pipes: A Tool Pin Diameter Perspective. *International Journal of Applied Engineering Research*, *14*(18), 3668-3677.

[35] Harwani, D. M., and Badheka, V. J. (2019). Effect of Shoulder Diameter on Friction Stir Welding of Al 6061 to SS 304. In *Innovations in Infrastructure* (pp. 355-366). Springer, Singapore.

[36] Ravikumar, S., Rao, V. S., and Pranesh, R. V. (2014). Evaluation of Ultimate Tensile Strength Parameters in Dissimilar Friction Stir Welded Joints Using Box-Behnken Experimental Design. *International Journal of Applied Engineering Research*, *9*(26), 9066-9071.

[37] Dyn, N., Levin, D., and Rippa, S. (1986). Numerical procedures for surface fitting of scattered data by radial functions. *SIAM Journal on Scientific and Statistical Computing*, *7*(2), 639-659.

[38] John, P. W. (1998). *Statistical design and analysis of experiments*. Society for Industrial and Applied Mathematics.

[39] Zadeh, L. A. (1965). Fuzzy sets, information and control. *vol*, *8*, 338-353.

[40] Takagi, T., and Sugeno, M. (1985). Fuzzy identification of systems and its applications to modeling and control. *IEEE transactions on systems, man, and cybernetics*, (1), 116-132.

[41] Van Leekwijck, W., and Kerre, E. E. (1999). Defuzzification: criteria and classification. *Fuzzy sets and systems*, *108*(2), 159-178.

[42] Edwards, J. R. (2007). Polynomial regression and response surface methodology. *Perspectives on organizational fit*, 361-372.

[43] Yen, J., Langari, R., and Zadeh, L. A. (Eds.). (1995). *Industrial applications of fuzzy logic and intelligent systems* (Vol. 1). New York: IEEE press.

[44] Shi, Y., Eberhart, R., and Chen, Y. (1999). Implementation of evolutionary fuzzy systems. *IEEE Transactions on fuzzy systems*, *7*(2), 109-119.

[45] Roychowdhury, S., and Pedrycz, W. (2001). A survey of defuzzification strategies. *International Journal of intelligent systems*, *16*(6), 679-695.

[46] Sabry, I., and El-Kassas, A. M. Comparative Study on Different Tool Geometrics in Friction Stirred Aluminum Welds Using Response Surface Methodology.

[47] Mas'ud, A. A., Ardila-Rey, J. A., Albarracín, R., Muhammad-Sukki, F., and Bani, N. A. (2017). Comparison of the performance of artificial neural networks and fuzzy logic for recognizing different partial discharge sources. *Energies*, *10*(7), 1060.